Low Noise Ultra-Flexible SiP Switching Platform for mmWave OCDM & Multi-Band OFDM ARoF Fronthaul

Devika Dass, *Graduate Student Member, IEEE*, Liang Yuan Dai, *Graduate Student Member, IEEE*, Keren Bergman, *Fellow, IEEE*, Xing Ouyang, *Member, IEEE*, Paul Townsend, *Member, IEEE*, Chris Roeloffzen, *Member, IEEE*, and Colm Browning, *Senior Member, IEEE*

***Abstract*— A highly flexible wavelength and space switched analog radio-over-fiber (ARoF) fronthaul transmission of a millimeter-wave (mmWave) emerging 6G waveform over a centralized/cloud radio access network (C-RAN) is experimentally demonstrated in this work. A spread spectrum multiplexing technique — orthogonal chirp division multiplexing (OCDM) — which is highly resilient to inter-channel interference and enables enhanced channel estimation is utilized in the fronthaul transmission demonstration. The flexible properties of a low noise silicon photonic (SiP) microring resonator (MRR) based tunable laser and a low cross-talk 4 × 4 SiP optical wavelength/space switch are combined to form a reconfigurable 10 km fronthaul system enabling 64-QAM OCDM transmission at 24 GHz with consistent performances ∼5% EVM across all test wavelengths/ports. A signal constituting Wi-Fi and 5G NR standard compatible 64-QAM orthogonal frequency division multiplexing (OFDM) bands, at 10 GHz and 24 GHz respectively, are also transmitted and evaluated in the proposed system with EVM performances below 64-QAM EVM limit (8%) achieved, thus demonstrating the system's potential in a future converged multi-service environment.**

***Index Terms*— SiP laser, SiP switch, ARoF, 6G, OCDM, 5G NR, Wi-Fi, OFDM, mmWave, C-RAN.**

I. Introduction

THE advent of beyond 5G and 6G technologies will necessitate the flow of massive volumes of information (10s or even 100s Gbps) through fixed and wireless broadband networks and extremely low latency for selective applications and connection between billions of devices and mobile users. Leveraging existing and future optical access network deployments to radio cell sites in a spectrally efficient, cost-effective and sustainable manner is critical [1]. With the recent standardization of the mmWave 5G New Radio (NR) Frequency Range 2 (FR2) band between 24-71 GHz for high throughput applications, the impact on radio access networks (RANs) is the densification of cell sites and deployed radio units (RUs). To this end, a centralized/cloud radio access network (C-RAN) approach is considered an indispensable solution enabling this densification of cell sites [2]. Moreover, its amalgamation with analog radio-over-fiber (ARoF) technology can immensely reduce the complexity of the RUs, making the cell sites more economical and thereby facilitating wide deployment. Considering the enormous volume of traffic and vast array of services expected from optical links between RUs and central office (CO), the advances in flexible optical networking technologies must be leveraged in C-RANs to provide a high-speed, sustainable and multi-vendor networking platform in support of current and emerging wireless technologies/ connectivity.

Highly wavelength flexible silicon photonic (SiP) integrated circuits can provide low noise, low crosstalk, high yield and small footprint when compared to discrete semiconductor components [3], and these advantages have been exploited by recent works focusing on RoF for C-RAN and converged service applications [4]. In [5], we demonstrated the transmission of multi-band intermediate frequency (IF) ARoF signals through a low cross-talk wavelength and space flexible SiP microring resonator (MRR) based optical switch. Xia et al. successfully deployed a similar SiP switch technology in support of a reconfigurable converged fixed and wireless network with digital RoF (DRoF) technology [6]. A Si_3N_4 MRR based reconfigurable optical add-drop multiplexer (ROADM) has been used in [7] to show the coexistence of multi-service mmWave ARoF and DRoF transmission in C-RAN, while a SiP MRR based smart edge in [8] enables the transmission of ARoF with wavelength division multiplexing in a converged optical access network scenario. This smart edge, located within the PON remote node, intercepts PON traffic and adds 5G signals to transmissions that are being sent to and from ONUs.

Manuscript received 27 February 2023; revised 18 April 2023; accepted 19 April 2023. Date of publication 24 April 2023; date of current version 9 May 2023. This work was supported in part by the Science Foundation Ireland (SFI) under Grant 18/SIRG/5579 and Grant SFI-12/RC/2276_P2_IPIC and in part by the Irish Research Council (IRC) under Grant GOIPD/2021/875 and Grant IRCLA/2022/3636. *(Corresponding author: Devika Dass.)*

Devika Dass and Colm Browning are with the School of Electronic Engineering, Dublin City University, Dublin 9, Ireland (e-mail: devika.dass2@mail.dcu.ie; colm.browning@dcu.ie).

Liang Yuan Dai and Keren Bergman are with the Department of Electrical Engineering, Columbia University, New York, NY 10027 USA (e-mail: ld2719@columbia.edu; bergman@ee.columbia.edu).

Xing Ouyang and Paul Townsend are with the Photonic Systems Group, Tyndall National Institute, Cork 021, T12 R5CP Ireland (e-mail: xing.ouyang@tyndall.ie; paul.townsend@tyndall.ie).

Chris Roeloffzen is with LioniX International BV, 7521 AN Enschede, The Netherlands (e-mail: c.g.h.roeloffzen@lionix-int.com).

Color versions of one or more figures in this letter are available at https://doi.org/10.1109/LPT.2023.3269901.

Digital Object Identifier 10.1109/LPT.2023.3269901

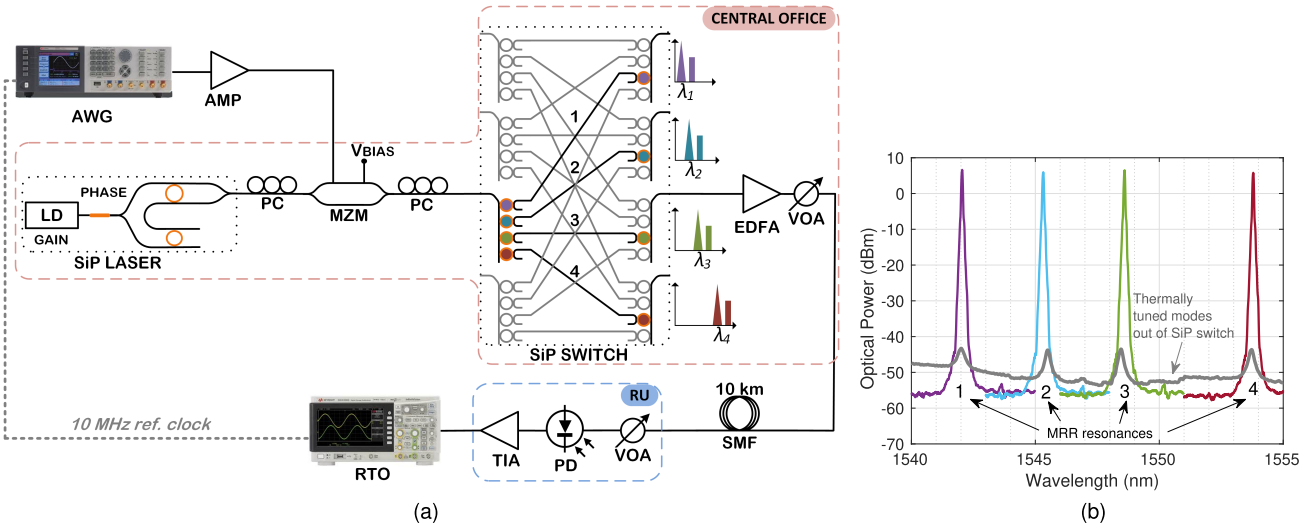

Fig. 1. (a) Experimental setup with tunable SiP based MRRs at the laser and switch (microheaters highlighted in orange), (b) shows the output of the laser tuned in turn to generate four wavelengths and the corresponding measured resonances of the four MRRs of SiP switch in this experiment (shown in grey).

In the wireless domain, much research effort is focussed on the development of new waveform designs that are resilient to harsh channel environments typically encountered at higher radio frequencies [9]. One such multi-carrier waveform is orthogonal chirp division multiplexing (OCDM) [10]. Through its use of a Fresnel transform (FnT), OCDM differs from the 5G waveform of choice – orthogonal frequency division multiplexing (OFDM) – such that information is encoded on a set of orthogonal chirps rather than frequency subcarriers. The signal's inherent spread-spectrum-like nature offers robustness to channel fading effects and Doppler shifts and it is seen as a promising candidate for next-generation mmWave mobile communications. OCDM also facilitates the use of chirp-based channel estimation (CE) and we have previously shown how this feature enables enhanced performance (compared to frequency domain CE) in an optical heterodyne/mmWave ARoF system [11].

In this work, we go beyond the state-of-the-art by constructing an ultra-flexible fronthaul system underpinned by the unique combination of a low noise SiN-InP MRR-based tunable laser source and a low crosstalk 4 × 4 SiP MRR-based optical wavelength/space switch for mmWave ARoF fronthaul provisioning with the emerging OCDM waveform. We also demonstrate the successful transmission of a multi-band OFDM signal constituting a narrowband signal resembling the 5G NR standard for mobile traffic and a wideband signal for broadband Wi-Fi service in the ultra-flexible ARoF fronthaul system, thus showing the system's viability in a multi-service environment.

II. OCDM/OFDM Transmission Over Ultra-Flexible SiP Laser & Switch Fabric

In the C-RAN architecture-based experimental setup, shown in Fig. 1a, the CO includes a widely tunable and low-noise TriPleX technology-based laser (a full description of the device is given in [12]). The laser consists of a gain section made of a semiconductor optical amplifier (SOA) and a cavity including a phase section and two Si_3N_4 MRRs (as highlighted

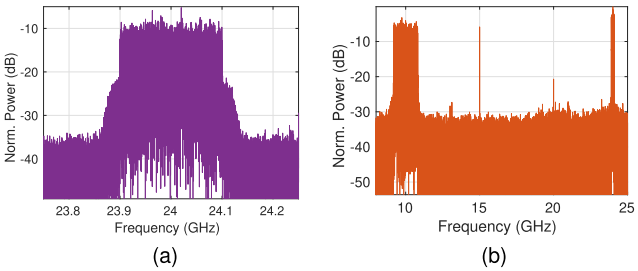

Fig. 2. Received electrical spectra of (a) 64-QAM OCDM at 24 GHz and (b) multi-band OFDM signal constituting Wi-Fi and 5G NR compatible signals at 10 GHz and 24 GHz respectively.

in orange in Fig. 1a) which are thermally controlled via microheaters. Control voltages to the microheaters associated with the two MRRs are used to tune the laser across the C-band. This widely tunable laser has a low relative intensity noise (∼−140 dB/Hz) and a narrow linewidth (∼40 kHz) at a gain current of 70 mA as reported in [12]. In this experiment, four separate wavelengths having ∼7 dBm optical power were used (spectra shown in Fig. 1b) with the laser's gain current set to 150 mA. The laser's output is modulated by two types of radio frequency (RF) signals via a Mach-Zehnder modulator (MZM) biased at quadrature. Utilizing the ARoF technique to modulate RF signals directly onto the optical carrier avoids digital/analog conversions while preserving the bandwidth efficiency and fidelity of the original RF data signal. This leads to improved system capacity and performance, making ARoF a desirable technique in future communication systems. The two types of software-generated signals are — (i) a single-band (SB) 64-QAM OCDM signal centered at 24 GHz (see Fig. 2a) and (ii) a multi-band (MB) 64-QAM OFDM signal consisting of 5G NR compatible signal at 24 GHz combined with a Wi-Fi compatible signal at 10 GHz (see Fig. 2b), whose detailed features are given in Table. I. A 60 GSa/s arbitrary waveform generator (AWG) is used to produce an RF signal for laser modulation via the MZM, thus generating a double sideband optical signal, which is then transmitted to a single port of

TABLE I
SB OCDM/OFDM AND MB OFDM SIGNAL PROPERTIES

Properties	OCDM/OFDM	MB-OFDM 5G NR	MB-OFDM Wi-Fi
(I)DFnT/(I)DFT[a]	1024	2048	2048
Symbol Rate	244.14 kHz	244.14 kHz	244.14 kHz
Chirps/Subcarrier	820	900	336
QAM-Level	64	64	64
Bandwidth	200.2 MHz	195.3 MHz	1.64 GHz
Data rate	1.2 Gbps	1.17 Gbps	9.84 Gbps
Carrier Frequency	24 GHz	24 GHz	10 GHz

[a]Inverse discrete Fresnel transform/Inverse discrete Fourier transform

the SiP MRR based 4 × 4 optical switch. The low crosstalk switch, whose design is depicted in the setup in Fig. 1a (see further details in [6]) allows all-optical transmission from a single input port to every output port through a designated MRR pair. Its operation is wavelength selective by appropriate thermal tuning of the resonances of each of the four MRR filters associated with each port. In the context of this C-RAN type demonstration, this functionally offers switch-and-select functionality for fronthaul transmission links to/from the CO. Combining this with the tuning capability of the laser provides a high degree of high bandwidth all-optical reconfigurability in the network.

In the example networking scenario implemented in this work, the resonant wavelength of the input and output MRR pairs associated with switch paths 1, 2, 3 and 4 (see Fig. 1a) were tuned to a configuration (see grey colored input MRR resonances in Fig. 1b). In this way, a connection from the input port to a particular output port is achieved by transmission of an associated wavelength across the C-band. In this scenario, each switch output port (representing connection to a separate fronthaul link served by the CO) can be addressed by appropriate tuning of the TriPleX hybrid integrated laser; thereby introducing an additional layer of networking flexibility on top of the wavelength/space switching capabilities of the SiP switch alone. This operation allows the optical transmitter/service at the CO to be connected to any local fronthaul link regardless of the SiP switch state.

The optical signal routed out of the switch port is amplified by an Erbium doped fiber amplifier (EDFA) to compensate for losses (∼10–15 dB) which are primarily attributed to coupling to/from the SiP chip. The edge coupling loss of 6 dB/facet is reported for a looped pair of MRRs [6]. Path-dependent losses are also introduced by on-chip bends in Si waveguides in the switch fabric and variations in the fabrication process. The output signal is then transmitted over 10 km of standard single mode fiber (SSMF). A variable optical attenuator (VOA) is utilized to regulate the optical power falling on a 40 GHz PIN photodetector (PD) with an integrated transimpedance amplifier (TIA), which is situated at the RU and responsible for converting the incident light into an electrical signal in this direct detection system. A 100 GSa/s real time oscilloscope (RTO) captures the electrical signal, which is then processed offline to evaluate the error vector magnitude (EVM) performance in all test cases i.e. all four configured switch paths/output ports.

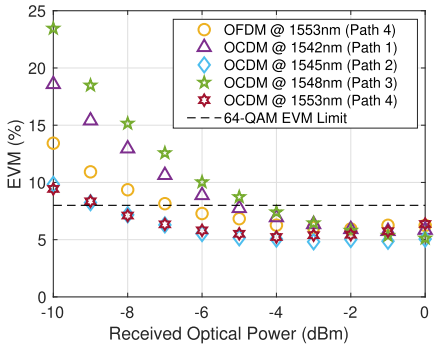

Fig. 3. EVM performance evaluation over varied optical power incident on PD.

III. RESULTS AND DISCUSSION

The received electrical spectrum of the transmitted 64-QAM OCDM signal via path 1 (at 1542 nm) is shown in Fig. 2a. The EVM performance is evaluated with respect to received optical powers (ROPs), shown in Fig. 3, for four wavelengths routed via four configured paths of the wavelength/space switch. EVM percentages below the 8% 64-QAM limit for ROPs higher than −5 dBm are observed, with the lowest EVM of 4.9% (bit error ratio (BER) of 3.2×10^{-5}) recorded for the 64-QAM OCDM signal received on the 1545 nm carrier (switch path 2) at a ROP of −1 dBm. Due to the switch path-dependent losses imposed by fabrication tolerances, coupling and bending losses from on-chip Si waveguides and slight thermal fluctuations impacting MRR tuning, signals traversing each switch path experience different losses, leading to a variation in optical power observed at each output port. This directly impacts the optical signal-to-noise ratio (OSNR) at each wavelength as signals at the output of the switch are fed to the booster EDFA, ultimately leading to the disparity in the performance curves presented in Fig. 3. This effect leads to a maximum receiver sensitivity degradation of 4 dB at the 8% EVM limit when comparing OCDM performances at 1548 nm (path 3) with that received at 1553 nm (path 4).

In all cases at higher ROPs i.e. from −3 to 0 dBm, the EVM performances converge to 5% as the limitations imposed by the optical receiver (shot noise and non-linearity) begin to dominate the system performance. The clear 64-QAM constellations of OCDM signals received at −2 dBm via the four tested SiP switch paths/wavelength conditions are color-coded with respect to the wavelengths and are shown in Fig. 4, indicate excellent performance. To compare OCDM with current 5G technology, an equivalent 24 GHz 1.2 Gbps 64-QAM OFDM mobile signal was also transmitted at 1553 nm and routed via switch path 4 with the same conditions as for the best performing OCDM signal for a fair comparison. In this case, where standard OFDM frequency domain channel estimation (CE) is utilized, the performance curve ("○" in Fig. 3) indicates a 2 dB degradation in receiver sensitivity with respect to OCDM (for the same networking conditions) at the 8% EVM limit. This result highlights the performance enhancement enabled through the use of OCDM's pulse compression-based CE technique [13], providing a superior channel estimation in this system dominated by Gaussian noise processes and

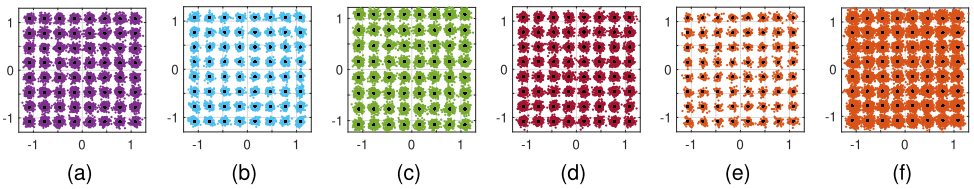

Fig. 4. Overlapped transmitted and received constellations of 64-QAM OCDM at four wavelengths, i.e. 1542 nm, 1545 nm, 1548 nm and 1553 nm, coming out of switch paths (a) 1, (b) 2, (c) 3 and (d) 4 respectively and the multi-band 64-QAM OFDM compatible to (e) 5G NR and (f) Wi-Fi standards at 1548 nm wavelength, all observed at ROP of −2 dBm incident on PD.

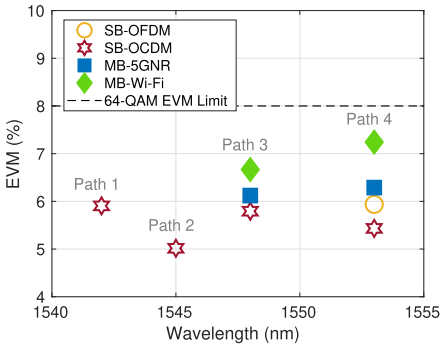

Fig. 5. EVM performance evaluation over wavelengths switched in C-band at −2 dBm ROP falling on PD.

is completely independent of the switch path the signal goes through.

We also transmitted a multi-band/multi-service ARoF signal composed of two wireless services; a narrowband 1.2 Gbps 64-QAM OFDM signal adhering to the 5G NR mobile standard at 24 GHz IF and a wideband 10 Gbps 64-QAM OFDM Wi-Fi standard compatible signal at 10 GHz IF. Fig. 2b shows the received electrical spectrum of the multi-band signal transmitted through path 3 in the optical switch. The EVM performance of the composite signal transmitted through switch paths 3 and 4, with a ROP of −2 dBm, is shown in Fig. 5. Best EVMs 6.1% and 6.6% are achieved for 5G NR and Wi-Fi services, respectively, through switch path 3 (carrier wavelength 1548 nm). This divergence in performance between the two services is also observed for transmission through switch path 4 and is to be expected given the relatively large bandwidth of the Wi-Fi service, compared to that of 5G NR (see Table I). The 0.4% EVM difference between SB-OFDM and SB-OCDM for path 4 in Fig. 5 is attributed to ambient temperature variance during the measurement, rather than channel or signal-dependent effects. The overlapped constellation of transmitted and received 5G NR and Wi-Fi signals are shown in Fig. 4e and 4f respectively. The overall EVM performance of multi-band OFDM signal at 1548 nm and 1553 nm wavelengths is well below the 64-QAM EVM limit.

IV. Conclusion

Optical reconfigurability in future access networks for beyond 5G/6G technology will be critical to the deployment of interoperable, energy-efficient and cost-effective networks. The results presented in this work demonstrate how wavelength/space flexible SiP components can be deployed in a C-RAN architecture to deliver all-optical fronthaul switching/routing directly from a RAN central office. Furthermore, the flexible SiP platform presented is shown to support ARoF transport of an emerging 6G waveform — OCDM — at mmWave frequencies with performances down to ∼5% in all test cases. The system is also shown to support dynamic multi-service delivery in a C-RAN network which will become a vital aspect of interoperability in future access networks. In the future, a potential improvement in energy efficiency can be achieved by implementing a feedback control system to stabilize the MRRs in the experiment. Overall, the proposed system and experimental results presented in this work highlight the potential for the key advantages of fully integrated SiP systems to be harnessed in support of the development of truly converged and flexible future access networks.

References

[1] M. Giordani, M. Polese, M. Mezzavilla, S. Rangan, and M. Zorzi, "Toward 6G networks: Use cases and technologies," *IEEE Commun. Mag.*, vol. 58, no. 3, pp. 55–61, Dec. 2020.

[2] N. Alliance. (2019). *5G RAN CU—DU Network Architecture, Transport Options and Dimensioning*. [Online]. Available: https://www.ngmn.org/wp-content/uploads/Publications/2019/190412_NGMN_RANFSX_D2a_v1.0.pdf

[3] P. Dong, Y.-K. Chen, G.-H. Duan, and D. T. Neilson, "Silicon photonic devices and integrated circuits," *Nanophotonics*, vol. 3, nos. 4–5, pp. 215–228, 2014.

[4] X. Guan, W. Shi, J. Liu, P. Tan, J. Slevinsky, and L. A. Rusch, "Silicon photonics in optical access networks for 5G communications," *IEEE Commun. Mag.*, vol. 59, no. 6, pp. 126–131, Jun. 2021.

[5] C. Browning et al., "A silicon photonic switching platform for flexible converged centralized-radio access networking," *J. Lightw. Technol.*, vol. 38, no. 19, pp. 5386–5392, Oct. 1, 2020.

[6] J. Xia et al., "A future proof reconfigurable wireless and fixed converged optical fronthaul network using silicon photonic switching strategies," *J. Lightw. Technol.*, vol. 41, no. 6, pp. 1610–1618, Mar. 15, 2023.

[7] E. Ruggeri et al., "Reconfigurable fiber wireless fronthaul with A-RoF and D-RoF co-existence through a Si_3N_4 ROADM for heterogeneous mmWave 5G C-RANs," *J. Lightw. Technol.*, vol. 40, no. 16, pp. 5514–5521, Aug. 15, 2022.

[8] X. Guan, R. Dubé-Demers, W. Shi, and L. A. Rusch, "Heterogeneous optical access networks: Enabling low-latency 5G services with a silicon photonic smart edge," *J. Lightw. Technol.*, vol. 39, no. 8, pp. 2348–2357, Apr. 15, 2021.

[9] M. Alsabah et al., "6G wireless communications networks: A comprehensive survey," *IEEE Access*, vol. 9, pp. 148191–148243, 2021.

[10] X. Ouyang and J. Zhao, "Orthogonal chirp division multiplexing," *IEEE Trans. Commun.*, vol. 64, no. 4, pp. 3946–3957, Sep. 2016.

[11] C. Browning, X. Ouyang, D. Dass, G. Talli, and P. Townsend, "Orthogonal chirp-division multiplexing for performance enhanced optical/millimeter-wave 5G/6G communications," in *Proc. Opt. Fiber Commun. Conf. (OFC)*, 2021, pp. 1–3.

[12] Y. Lin et al., "Characterization of hybrid InP-TriPleX photonic integrated tunable lasers based on silicon nitride (Si_3N_4/SiO_2) microring resonators for optical coherent system," *IEEE Photon. J.*, vol. 10, no. 3, pp. 1–8, Jun. 2018.

[13] X. Ouyang, C. Antony, G. Talli, and P. D. Townsend, "Robust channel estimation for coherent optical orthogonal chirp-division multiplexing with pulse compression and noise rejection," *J. Lightw. Technol.*, vol. 36, no. 23, pp. 5600–5610, Dec. 1, 2018.